IOP Publishing Nanotechnology
Nanotechnology 26 (2015) 195103 (13pp) doi:10.1088/0957-4484/26/19/195103

Source of cytotoxicity in a colloidal silver nanoparticle suspension

Manolya Kukut Hatipoglu[1], Seda Keleştemur[1], Mine Altunbek[1] and Mustafa Culha

Department of Genetics and Bioengineering, Faculty of Engineering, Yeditepe University, Ataşehir, Istanbul 34755, Turkey

E-mail: mculha@yeditepe.edu.tr

Received 19 February 2015, revised 16 March 2015
Accepted for publication 17 March 2015
Published 23 April 2015

Abstract

Silver nanoparticles (AgNPs) are increasingly used in a variety of applications because of their potential antimicrobial activity and their plasmonic and conductivity properties. In this study, we investigated the source of cytotoxicity, genotoxicity, and reactive oxygen species (ROS) production on human dermal fibroblast and human lung cancer (A549) cell lines upon exposure to AgNP colloidal suspensions prepared with the simplest and most commonly used Lee–Meisel method with a variety of reaction times and the concentrations of the reducing agent. The AgNPs synthesized with shorter reaction times were more cytotoxic and genotoxic due to the presence of a few nanometer-sized AgNP seeds. The suspensions prepared with an increased citrate concentration were not cytotoxic, but they induced more ROS generation on A549 cells due to the high citrate concentration. The genotoxicity of the suspension decreased significantly at the higher citrate concentrations. The analysis of both transmission electron microscopy images from the dried droplet areas of the colloidal suspensions and toxicity data indicated that the AgNP seeds were the major source of toxicity. The completion of the nucleation step and the formation of larger AgNPs effectively decreased the toxicity.

Keywords: silver nanoparticles, citrate concentration, reaction time, cytotoxicity, genotoxicity

(Some figures may appear in colour only in the online journal)

1. Introduction

In recent years, the possible adverse effects of nanomaterials (NMs) on human health and the environment have become a major concern. Thus, a considerable effort has been underway to clarify public worries. In this regard, several approaches have been proposed to reduce the toxicity of these novel materials. One approach is to modify the surface chemistry of NMs with a biocompatible molecule or polymer [10, 12, 15, 19, 36]. However, this approach may not be a complete solution since not all NMs are suitable for surface modifications. Additional problems include the instability of the surface modifier and the NMs and changes in the physicochemical properties of the NMs as a result of surface modification. Another approach is to consider synthesis methods, physicochemical properties, and the adverse effects of the NMs from the beginning, which is called 'safety by design' [43].

The use of noble metal nanoparticles such as gold and silver (AuNPs and AgNPs) has been widely investigated for potential applications in numerous products, ranging from medical devices to electronics, due to their unique plasmonic and other physicochemical properties [1, 31]. AgNPs are generally used in consumer products due to their antibacterial and wound-healing properties [23]. The potential use of AgNPs has also been intensively investigated in optoelectronics, biosensors, catalysis, and inks [23, 30, 35, 44].

The most common method for preparing AgNPs is wet synthesis, and a vast number of synthesis procedures are available in the literature [8, 16, 21, 25, 28, 32, 34, 37, 42]. In these methods, silver ions from its soluble salts are reduced with a reducing agent such as borohydride [32], citrate [21], ascorbate [28], elemental hydrogen [7], or polyvinylpyrrolidone (PVP) [8]. Among these methods, the

[1] These authors contributed equally.

 © 2015 IOP Publishing Ltd Printed in the UK

citrate-based reduction method, known as Lee-Meisel method, is the one most commonly used to synthesize spherical AgNPs with a thin capping layer of citrate ions on their surfaces [21]. Although the size and shape of the AgNPs can be controlled to some degree, the polydispersity in shape and size is still a major problem, as it is in most wet synthesis methods. This is due to the difficulty of controlling the nucleation step and the growth of the AgNPs with regard to the reactivity of silver precursor seeds [39].

One of the difficulties of a healthy evaluation of the toxicity of most NMs is the variation in their preparation, which results in different sizes, shapes, surface chemistry, and polydispersity. For example, there are conflicting results in the literature concerning the toxicity of AgNPs [11, 18, 24]. Smaller-sized AgNPs were reported to be more toxic due to their rapid release of Ag^+ ions [11, 24]. On the contrary, large AgNPs (100 nm) were reported to induce the highest toxicity in another study (10 nm versus 100 nm) [18]. Therefore, the modification through the Ag-S bond may help to reduce toxicity by controlling ion release and blocking the active surface area [13, 36]. In addition, it has been suggested that coating the AgNP surfaces with a molecule of biological origin might help to increase the possibility of their use in medical applications such as cancer phototherapy and wound healing [17, 36]. However, incomplete surface coverage of ligands or loss of the surface coating after the modifications may not completely prevent the release of Ag^+ ions [40]. Haase *et al* found that AgNPs still continued to release Ag^+ ions and to be toxic after being coating with a peptide [13]. As seen from the reports mentioned above, the source of the toxicity is mainly attributed to the release of Ag^+ ions from the NPs. However, it is also possible that the AgNPs uptaken by the cell can cause adverse effects by coming into contact with cellular components [41]. Although the release of Ag^+ ions is a major source of toxicity in the long term, it is not clear what causes the toxicity in the short term when all Ag^+ ions are reduced to AgNPs in a suspension.

In this study, we investigated the source of toxicity from an AgNP colloidal suspension prepared using the Lee–Meisel method [21]. The reduction time of the Ag^+ ions to AgNPs and the reductant concentrations varied; the resulting suspensions were monitored for AgNP size variation with ultraviolet-visible (UV-vis) spectroscopy, dynamic light scattering (DLS), and transmission electron microscopy (TEM). The colloidal suspensions prepared under varying conditions were tested for cell viability, reactive oxygen species (ROS) generation, and genotoxicity *in vitro* conditions in order to identify the source of toxicity, with the goal of preparing a less-toxic AgNP colloidal suspension.

2. Experimental

2.1. Materials

Silver nitrate ($AgNO_3$) was purchased from Sigma-Aldrich (Germany). Trisodium citrate-dihydrate, hydrochloric acid (HCl, 37%), and nitric acid (HNO_3, 65%) were purchased from Merck-Millipore (Germany). All reagents were used as purchased, without further purification. Water used in the experiments was purified by the Milli-Q system to a resistivity of 15.5 mΩ cm. Dulbecco's Modified Eagle's Medium (DMEM), DMEM F-12 Ham, and fetal bovine serum (FBS) were purchased from Sigma-Aldrich (Germany). L-glutamine and penicillin were purchased from Gibco (UK). A WST-1 assay kit was purchased from Roche Diagnostic GmbH (Germany). A DCFDA assay kit was purchased from Abcam (UK).

2.2. Synthesis of AgNPs

The AgNP colloidal suspensions were prepared by modifying the Lee-Meisel method [21] in two ways: by varying the reaction time and the citrate concentration. All glassware was washed with a mixture of HCl: HNO_3 (70:30) (v/v) before use.

In the first experiment, the boiling time was gradually increased while keeping the $AgNO_3$ and citrate concentrations constant. Eighteen mg of $AgNO_3$ was dissolved in 98 mL ddH_2O, and the $AgNO_3$ solution was heated until boiling while stirring. Then, 2.0 mL (1%) of sodium citrate solution was added dropwise, and the final volumes were adjusted to 100 mL. The reaction was quenched at increasing times from 5 to 50 min by cooling in an ice-water bath.

In the second experiment, the AgNPs were synthesized by varying the sodium citrate concentration while keeping the boiling time and the $AgNO_3$ concentration constant. Eighteen mg of $AgNO_3$ was dissolved in 92–99.5 mL ddH_2O (depending on the trisodium citrate amount to be added) and heated until boiling. Then, increasing volumes of citrate solution (1%), from 0.5 to 8.0 mL, were added dropwise, and the final volumes were adjusted to 100 mL. The final citrate concentration range was between 2×10^{-4} M and 64×10^{-4} M. The reactions were quenched by cooling the reaction mixture in an ice-water bath at 50 min.

2.3. Characterization of synthesized AgNPs

The UV-vis spectra were obtained using a spectrophotometer (Lambda 25, Perkin Elmer). The size distribution of the AgNPs was determined using DLS (Nanozetasizer, Malvern) at 25 °C, using samples appropriately diluted with ddH_2O. The TEM analysis of AgNPs was performed with a JEOL-2100 TEM instrument equipped with an Oxford Instruments 6498 EDS system (Germany). The operating voltage was 200 kV (LaB6 filament).

2.4. Cytotoxicity assessments

Human dermal fibroblast (HDF) cells and human lung carcinoma epithelial cells (A549 cells) were used for the cytotoxicity assessments of the AgNPs. HDF cells were grown in DMEM high glucose, supplemented with 10% FBS, 100 unit mL^{-1} penicillin, and 100 unit mL^{-1} streptomycin. A549 cells were grown in DMEM F-12 Ham supplemented with 10% FBS, 100 unit mL^{-1} penicillin, 100 unit mL^{-1} streptomycin,

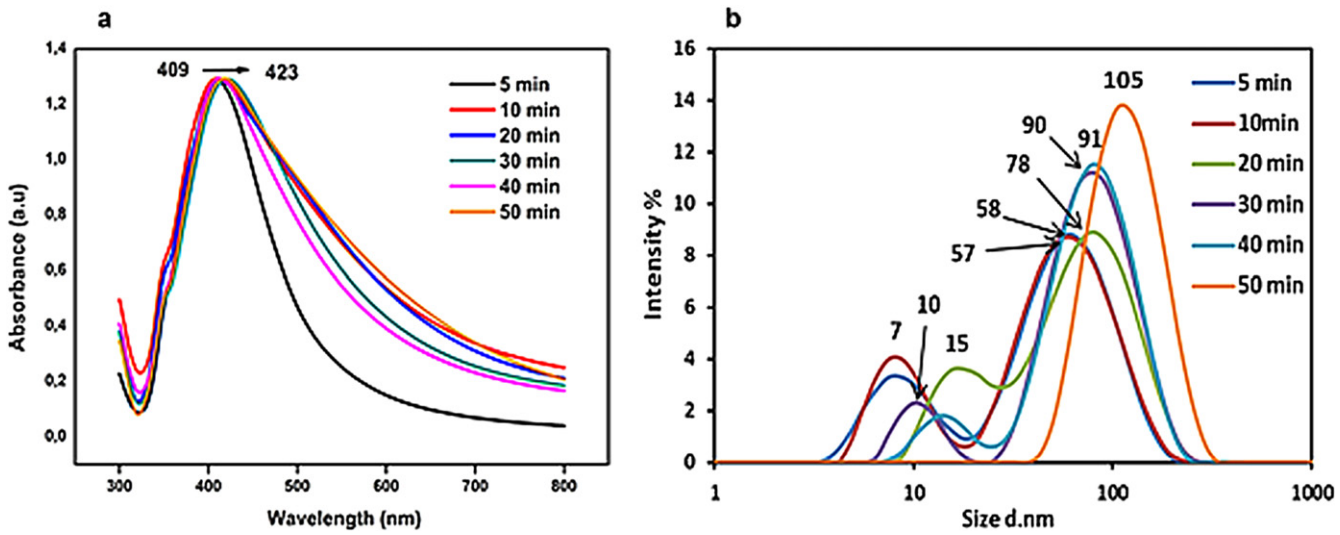

Figure 1. UV-Vis (a) and DLS spectra (b) of AgNPs prepared with increasing reaction time from 5 min to 50 min. The data shown are the mean of triplicates.

and 2 mM L-glutamine. Both cell types were incubated at 37 °C in a humidified incubator with 5% CO_2.

The cytotoxicity of the AgNPs was evaluated by WST-1 assay, through measuring mitochondrial activity. The cells were seeded in a 96-well plate and grown to 80–90% confluence before AgNP exposure. The cells were treated with the AgNPs in a 12.5–100.0 μg mL^{-1} concentration range for 24 h. Nontreated cells were used as a control. After 24 h exposure, the cytotoxicity of the AgNPs was assessed with a WST-1 assay. Briefly, the cell culture medium was removed from the 96-well plate and the cells were washed with PBS to remove residual AgNPs from the wells. Then, fresh medium containing 10% WST-1 solution was added to the wells and the cells were incubated for 1 h. The formed formazan medium was placed into a new 96-well plate to avoid the interference of any AgNPs remaining inside the cells or on the cell surfaces with the formazan absorbance. The absorbance of the formazan was measured at 450 nm using an automated plate reader (KC Junior Software, Elx80). The data were normalized to control values (no particle exposure), which were set at 100% cell viability. The cytotoxicity assessment was repeated three times with AgNPs synthesized in three batches.

The cytotoxicity of possible factors such as unreduced Ag^+ ions and AgNP seeds remaining in the supernatant was evaluated after removing the AgNPs from the supernatant by precipitating via centrifugation at 5500 rpm for 50 min. The supernatant cytotoxicity was evaluated by adjusting the volumes as they were applied during the AgNPs' cytotoxicity assessment. After 24 h exposure, the cell viability was evaluated with a WST-1 assay.

2.5. Reactive oxygen species generation

The ROS generation of HDF and A549 cells was measured with the DCFH-DA assay after exposure to the AgNPs. Briefly, the HDF and A549 cells were grown to 80–90% confluence in a 96-well plate. Before the NP addition, the cells were incubated with 20 μM DCFDA solution for 45 min at 37 °C in a humidified incubator with 5% CO_2 under light protection. Then, the cells were treated with suspensions containing AgNPs in a 5–25 μg mL^{-1} concentration range. After the nanoparticle addition, the initial fluorescence of the plate was recorded with the excitation wavelength at 485 nm and the emission wavelength at 535 nm using a SpectraMax Paradigm Multi-Mode Microplate Reader (SoftMax® Pro Software). After 6 h incubating the cells with the AgNPs, the fluorescence was recorded under the same conditions. Initial fluorescence was used as background. Tert-butyl hydrogen peroxide was used as a positive control.

2.6. Genotoxicity assessments

The genotoxicity of the AgNPs was assessed after exposure of A549 cells to 25 μg ml^{-1} AgNPs for 24 h through alkaline single-cell gel electrophoresis. Following AgNP exposure, the cells were embedded within 0.65% low-melting agarose onto high-melting-agorose-coated slides that had been refrigerated at 4 °C for 30 min. Then, the slides were placed into a lysis solution (1% Triton X, 10% DMSO, 2.5 M NaCl , 0.1 EDTA, 10 mM Tris base, pH 10) for 1 h at 4 °C. DNA was denatured with alkaline buffer for 40 min. Then, electrophoresis was performed on the slides at 25 V and 300 mA for 20 min with an alkaline buffer. The slides were immersed in a neutralization buffer solution (0.5 M Tris-HCl, pH 7.5) for 15 min at 4 °C. The cells were fixed into 70% ethanol for 10 min. The DNA was stained with SYBR green dye at 4 °C for 30 min. After these processes, the comet assay images were acquired with florescence microscopy, and the tail moment of the DNA was measured by comet image analysis (Perceptive Instruments, Comet IV). Fifty comets were analyzed per modified particles.

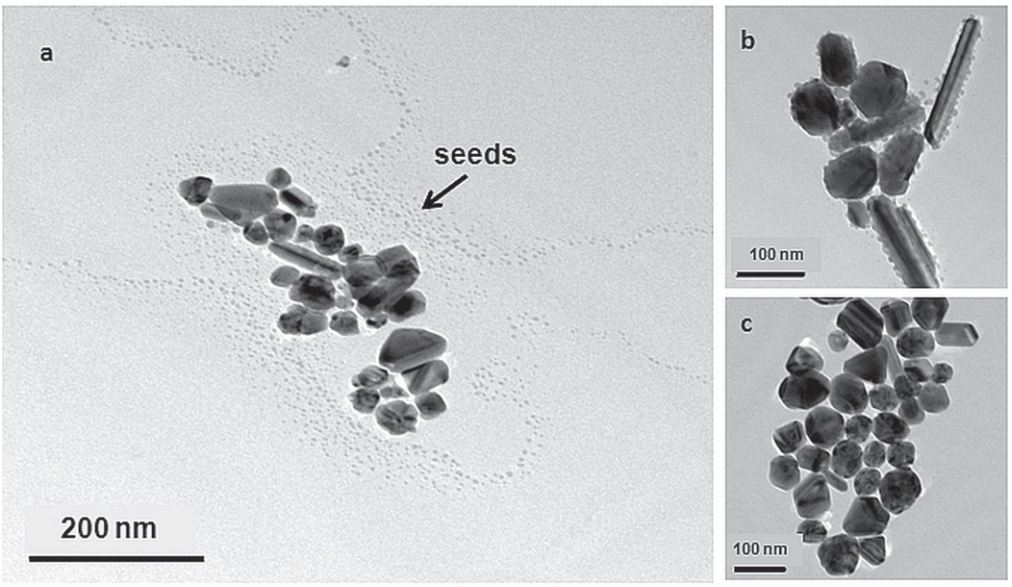

Figure 2. TEM images of AgNPs prepared at increasing reaction times (a) 5 min, (b) 20 min and (c) 50 min.

3. Results

The influence of the reaction termination time on the reduction of Ag^+ ions into AgNPs was investigated by quenching the reaction mixture in an ice-water bath for 5 to 50 min. Figure 1(a) shows the UV-vis spectra of the AgNP colloidal suspensions at increasing reaction times. A gradual up-shift in the absorbance maximum of the UV-vis spectra of the colloidal suspensions from 409 to 423 nm was observed as the reaction time increased, indicating the size growth of the AgNPs. However, the shape of the absorbance curve broadens as the reaction time increases, suggesting that a few larger AgNPs are forming with the increasing reaction time. The changes in the size of AgNPs were also monitored with DLS, as shown in figure 1(b). Although most of the AgNPs are in the range of 60–105 nm, there are a small number of AgNPs ranging from 8 to 15 nm hydrodynamic sizes when the reaction is interrupted before 50 min. As the reaction time increases, the hydrodynamic sizes of those smaller AgNPs become larger, but when the reaction is stopped at 50 min, the small-seed AgNPs disappear, indicating their fusion into larger AgNPs.

Further, the TEM images, which were used to examine the particle size and morphology, were acquired from the dried droplet areas of the colloidal suspensions of the reactions terminated at increasing reaction times. Figure 2 shows the TEM images of the AgNPs after 5, 20, and 50 min. The presence of large AgNPs up to 60 nm even after 5 min indicates that the larger AgNPs form rather fast. However, many small AgNPs, with an average size of 5 nm, were clearly visible around the larger AgNPs on the TEM images seen in figure 2(a). These small AgNPs were considered to be the seeds. When the reaction time was increased to 20 min, there were still seeds only on the surface of the large AgNPs (figure 2(b)), indicating their fusion to the large AgNPs in their growth progress. Figure 2(c) shows the TEM image of AgNPs at 50 min. As one can see, there are no unfused seeds left either around the AgNPs or on their surfaces. From these observations, one can conclude that the AgNP seeds continue to fuse with the other seeds and the larger AgNPs as the reaction progresses. However, the number of AgNPs seeds decreased with the increasing reaction time, since all Ag^+ ions were consumed with their reduction. This hypothesis supports the band shapes and shifts on the UV-vis and size distributions on the DLS spectra of the colloidal suspensions obtained at increasing reaction times. Even at the 5 min termination, the presence of a small fraction of large particles, along with many seeds, allows us to obtain a UV-vis spectrum similar to the spectra obtained from the suspensions with increased reaction times. However, the UV-vis spectra of the suspension terminated at 5 min is noticeably narrower, suggesting incomplete AgNP formation.

In the second part of the study, the effect of sodium citrate concentration on the reaction outcome was evaluated. Figure 3(a) shows the UV-vis spectra of the AgNP suspension obtained at increased citrate concentrations from 2×10^{-4} M to 64×10^{-4} M. At lower citrate concentrations—2×10^{-4} and 4×10^{-4} M—a broadening of the UV-vis spectra was observed, indicating the formation of very large AgNPs and aggregates due to incomplete surface coverage of the AgNPs by citrate ions. The AgNP suspensions obtained at these lower concentrations were unstable, and the AgNPs from the suspension precipitated in about 24 h after the synthesis. When the citrate concentration was increased, the UV-vis spectrum became narrower and a significant blue shift from 554 nm to 441 nm was observed, indicating a decrease in the size of the AgNPs. The size of the particles was also monitored by DLS, as shown in figure 3(b). At lower citrate concentrations, the presence of a range of large particles is evident from both UV-vis and DLS spectra. As the citrate concentration increases, the large

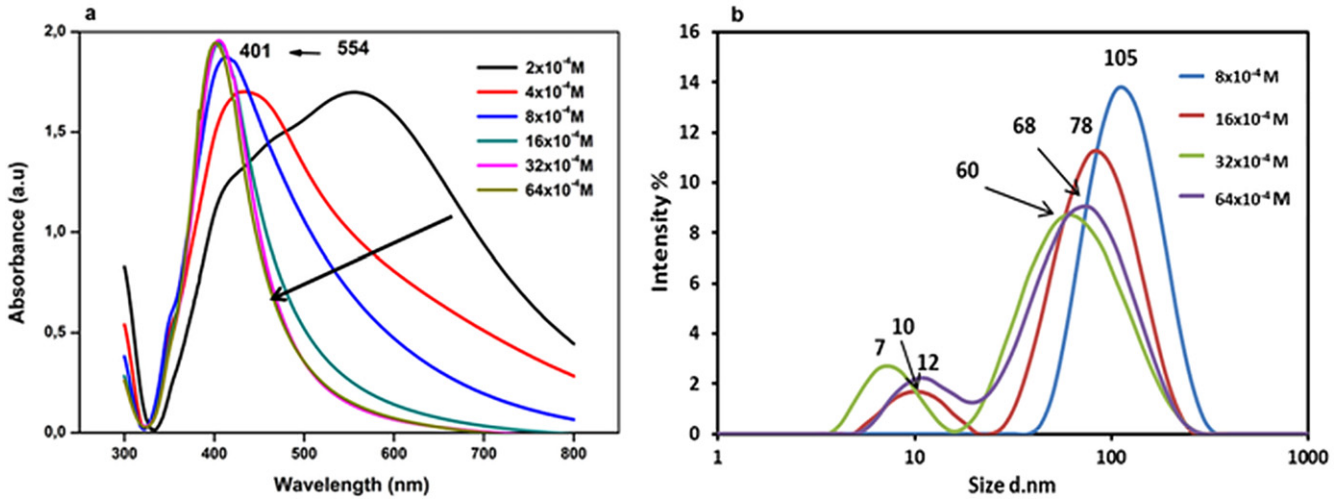

Figure 3. UV-Vis (a) and DLS spectra (b) of AgNPs prepared at increasing citrate concentrations. The data shown are the mean of triplicate measurements.

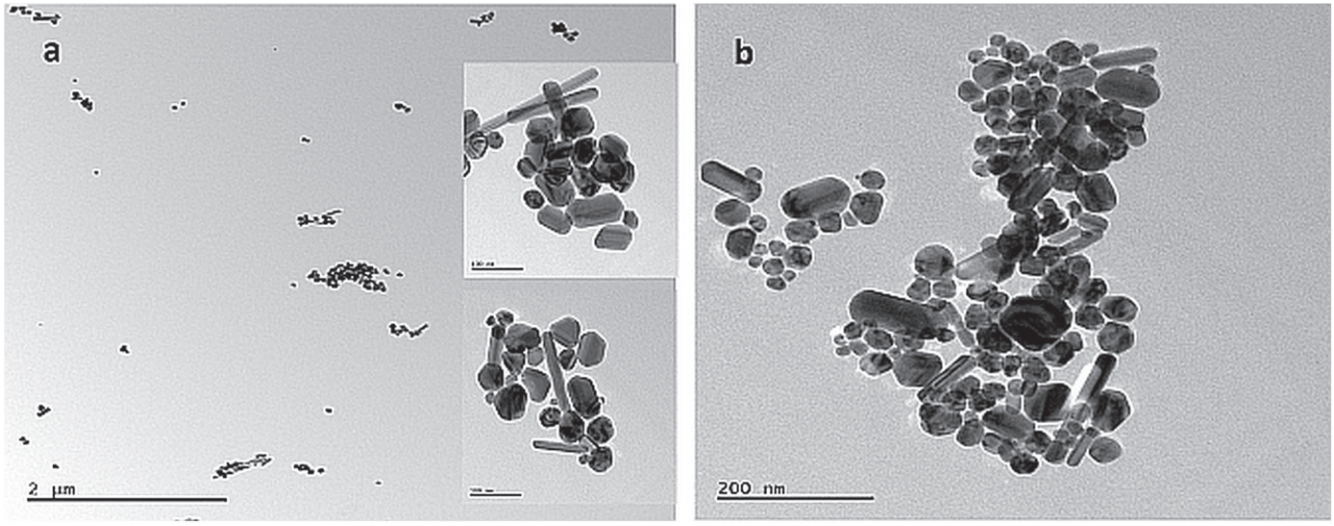

Figure 4. TEM images of AgNPs prepared at citrate concentrations of (a) 32×10^{-4} M and (b) 64×10^{-4} M.

range becomes narrower since citrate ions coat the AgNP surfaces and stabilize them.

The droplet areas of the AgNP colloidal suspensions were also examined with TEM. Figures 4(a) and (b) show the representative TEM images of the areas at citrate concentrations of 32×10^{-4} and 64×10^{-4} M, respectively. The colloidal suspensions prepared at the lower citrate concentrations were not imaged since they did not generate stable suspensions. Consistent with the DLS results, both small and large AgNPs were observed on the droplet areas of the colloidal suspensions at higher citrate concentrations. However, the average size of the AgNPs slightly decreased as the citrate concentration increased; the average size of the AgNPs was 25 nm with a citrate concentration of 32×10^{-4} M (figure 4(a)) and 20 nm with a citrate concentration of 64×10^{-4} M (figure 4(b)). There was no indication of AgNP seeds of a few nanometers in the dried droplet areas.

3.1. Cytotoxicity assessment

HDF and A549 cells were used in this study to investigate the adverse effects of the prepared AgNP colloidal suspensions. A 12.5–100 μg mL^{-1} concentration range was selected to evaluate the cytotoxicity of the prepared AgNPs and to compare the results with previous *in vitro* reports [11, 22, 36]. The cytotoxicity was evaluated by measuring the mitochondrial activity after exposing the cells to the AgNPs for 24 h. To identify the possible source of the cytotoxicity, the supernatants of the centrifuged suspension were also tested for cell viability. The AgNPs were separated from the suspension with centrifugation, and very small AgNPs or seeds, along with the Ag^+ ions, could still remain in the supernatant; they may contribute to the overall toxicity of the colloidal suspension. Figure 5 shows the cell viability after exposing the cell to the AgNPs synthesized at increasing reaction times (from 5 min to 50 min) and the supernatant of the centrifuged respective suspensions for both cell lines (figures 5(a) and (a′)

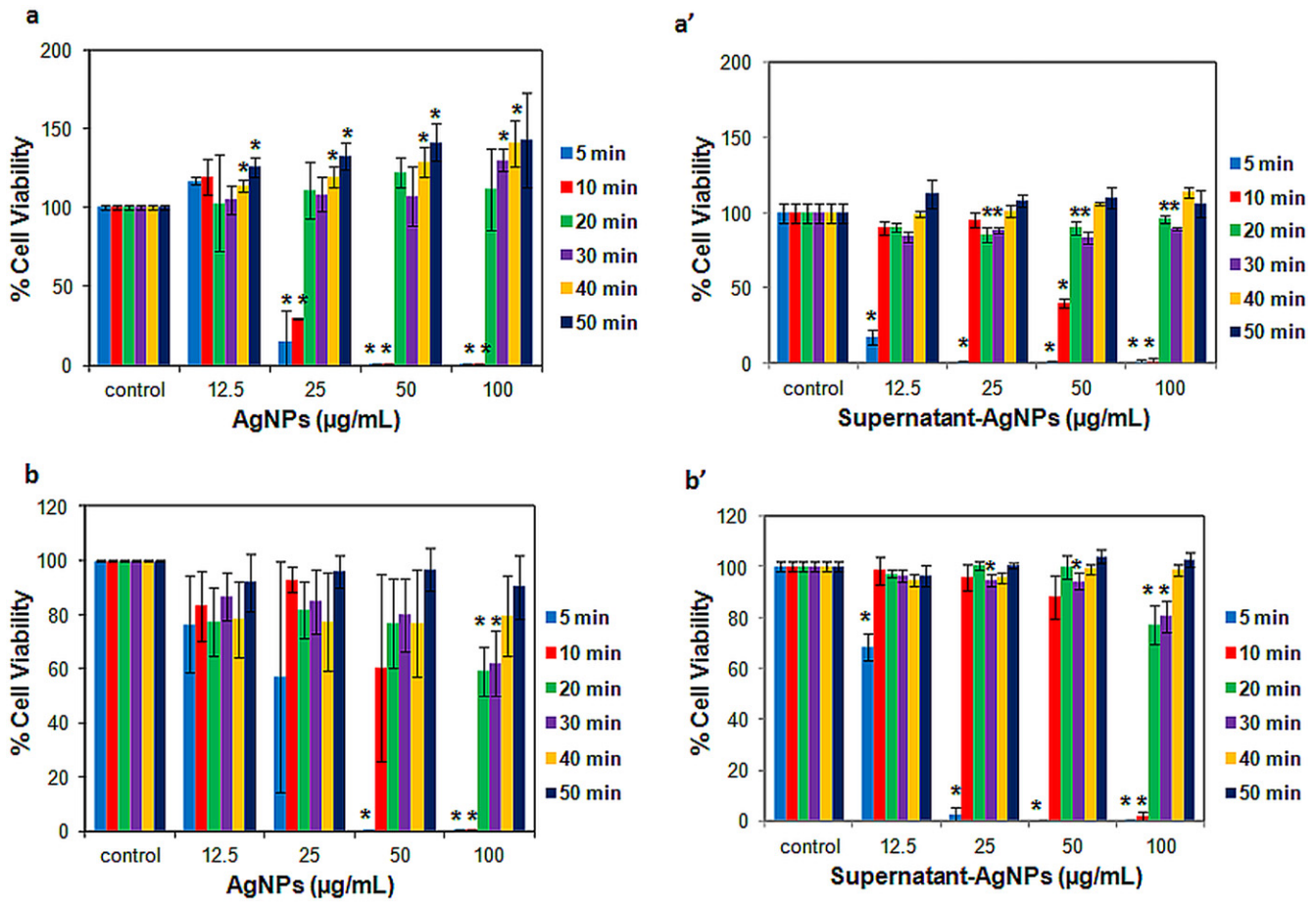

Figure 5. Cytotoxicity of AgNP colloidal suspensions (a and b) and their respective supernatants (a′ and b′) prepared with increasing reaction time from 5 to 50 min for 24 h treatment of HDF (a and a′) and A549 (b and b′) cell lines. The data normalized to control values (no particle exposure), which were set as 100% cell viability. * Shows the significant results compared to the control $P < 0.05$ as obtained using Student's t-test.

for HDF cells and figures 5(b) and (b′) for A549 cells). As seen in figure 5(a), HDF cell viability was not influenced at the 12.5 μg mL^{-1} concentration exposure to the AgNPs prepared in 5- and 10 min reactions. However, the exposure of 25 μg mL^{-1} AgNPs reduced the cell viability to 15% and 30% for the 5- and 10 min reactions, respectively, while a complete loss in cell viability was observed at higher AgNP concentrations. The reason behind the cytotoxicity of AgNPs prepared in early reaction times could be explained by numerous AgNPs seeds (figure 2(a)) having reactive surfaces, which also have the tendency to release Ag^+ ions in the culture medium and inside the cell. HDF cell viability was not influenced after exposure to the AgNPs prepared with 20- and 30 min reaction times for all concentration exposures. However, exposure to the AgNPs prepared at 40- and 50 min reaction times increased the HDF cell viability significantly compared to the nontreated control cells for all exposure concentrations.

The potential impact of the supernatant of the AgNPs (prepared via the increasing reaction times from 5 to 50 min) on HDF cell viability is presented in figure 5(a′). Cell viability was decreased to 17% after exposure of the supernatant of the AgNPs prepared at 5 min reactions at 12.5 μg mL^{-1} concentration. The exposure to higher than 12.5 μg mL^{-1} concentrations completely inhibited cell viability, which indicated the AgNP seeds' toxicity. The supernatant of the AgNPs prepared via 10 min reactions decreased cell viability almost 10% up to 50 μg mL^{-1} concentration exposures. The exposure of the supernatant from the AgNPs prepared at 10 min reactions at 50 μg mL^{-1} reduced the cell viability to 50%, while the 100 μg mL^{-1} exposure caused complete loss of viability. The supernatant of the AgNPs prepared at 20 and 30 min caused the loss of 10% cell viability.

The viability of A549 cells exposed to AgNP colloidal suspensions with increasing reaction times and their respective supernatants is shown in figures 5(b) and (b′), respectively. As seen in figure 5(b), the cell viability decreased to 70% and 15% after the 12.5 and 25 μg mL^{-1} concentration exposures, respectively, to the AgNPs prepared at 5 min. However, cell viability was completely lost with higher concentration exposures. This result is in agreement with the observations of HDF cells, which suggests that the seeds are the source of the toxicity. The AgNPs prepared at 10 min decreased cell viability almost 10% up to 50 μg mL^{-1} exposure, while the cell viability decreased about 60% at the 50 μg mL^{-1} exposure. Further, viability was completely lost at

100 μg mL^{-1} exposure. The high standard deviations in the cell viability results are due to the average cell viability results of three different batches of the AgNPs, where the nucleation step of the AgNP seeds may vary. The cell viability exposed to the AgNPs prepared at both 20- and 30 min reaction times did not show significant differences relative to each other, so the viability was about 75% for all concentration exposures. The observed average cell viability was 95% after exposure to the AgNPs prepared at 40- and 50 min reaction times. The decreased cytotoxicity of the AgNPs prepared in the increased reaction times was caused by the completion of the nucleation step, as it was in the case in the HDF cells.

Figure 5(b′) shows the A549 cell viability after exposure to the supernatant of the AgNPs prepared with increasing reaction times. Cell viability decreased to 70% with the exposure of the supernatant of the AgNPs prepared at 5 min at 12.5 μg mL^{-1} concentration, while cell viability was completely lost after higher concentration exposures. Cell viability did not change after exposure to the supernatant of the AgNPs prepared between 10- and 50 min reaction times, up to 50 μg mL^{-1} concentration. However, cell viability was completely lost after exposure to the supernatant of the AgNPs prepared at a 10 min reaction time at 100 μg mL^{-1} concentration. The supernatants from the AgNPs prepared at 20- and 30 min reaction times at 100 μg mL^{-1} concentration exposure caused a 20% loss in cell viability. Cell viability did not change after exposure to the supernatants from the colloidal suspensions prepared with 40- and 50 min reaction times. Although the HDF and A549 cell viability results vary, one can conclude that the source of the cytotoxicity is the AgNP seeds.

The influence of the AgNPs prepared by increasing the citrate concentration and their supernatant on cytotoxicity were shown on figure 6. The cell viability was not significantly affected after exposure of the AgNPs prepared between 16×10^{-4} M and 64×10^{-4} M citrate concentrations on both cell lines, as seen in figures 6(a) and (b). This can be explained by the completion of the formation of the AgNPs in 50 min, as was discussed above. Although the sizes of the AgNPs get smaller (figure 4) as the citrate concentration is increased, the cytotoxicity of the AgNP suspension does not change and remains nontoxic. The supernatant toxicity of the AgNPs prepared with increasing reaction times is shown in figures 6(a′) and (b′) for HDF and A549 cells, respectively. As one can see, remaining in the supernatant did not influence the HDF cells' viability. However, the A549 cell viability decreased to 90% after exposure to the supernatant of the AgNPs prepared by both 32.0×10^{-4} and 64.0×10^{-4} M citrate concentrations.

3.2. Reactive oxygen species generation

The role of intracellular ROS on the decrease in cell viability after the exposure to synthesized AgNPs was evaluated with a DCFDA assay by measuring DCF (2′, 7′-dichlorofluorescein) fluorescence converted from DCFDA (2′, 7′–dichlorofluorescein diacetate) on ROS production by AgNP-exposed cells. Tert-butyl hydrogen peroxide was used as positive control (PC) for the oxidation of DCFDA. The DCF produced by the AgNPs was calculated from the relative fluorescence intensity of the PC. Untreated cells were used as a negative control, in which the DCF fluorescence was not observed (data not shown). Figures 7(a) and (a′) show the ROS production of HDF cells after exposure to AgNPs synthesized with increasing reaction times and their supernatant, respectively. As seen in figure 7(a), the intensity of DCF was about 15% produced by HDF cells after exposure to AgNPs prepared with 5- to 30 min reaction times. However, ROS production was not observed after exposure to the AgNPs prepared with 40- and 50 min reaction times. The reason for the decreased ROS production after the exposure of both cells to the AgNP suspensions prepared at 40 and 50 min can be explained by the decreased reactive surface that results from the depletion of the seeds in the colloidal suspension as the reaction time increases.

The ROS production of the both cells with exposure to AgNP colloids prepared at increased citrate concentration is shown in figure 8. The ROS production was not induced by the exposure of the AgNP colloids prepared at increased citrate concentrations nor by their supernatants on HDF cells, as seen in figures 8(a) and (a′), respectively. However, A549 cells produced 30% ROS upon exposure to the AgNPs prepared up to 32×10^{-4} M citrate. Increasing the citrate concentration to 64×10^{-4} M increased the ROS production to 150%, which was much more than positive control. The supernatant of the AgNPs prepared between 8 and 32×10^{-4} M also induced the ROS production on A549 cells of about 15%. However, the AgNP colloidal suspension prepared with 64×10^{-4} M citrate induced 85% ROS production on A549 cells, demonstrating the influence of the citrate ions on A549 cells.

3.3. Genotoxicity

The DNA damage to A549 cells upon exposure to the AgNP colloidal suspension at 25 μg mL^{-1} concentration was evaluated with a comet assay. As seen in figure 9(a), there was no significant difference in the caused DNA damage between the AgNPs prepared with increased reaction times. In all cases, the DNA tail moment was measured as 25 μm. In addition, the supernatant of these AgNPs showed similar DNA damage to A549 cells, except the AgNPs prepared at 50 min. The DNA tail moment decreased to 10 μm after the exposure to the supernatant of the AgNPs prepared at 50 min. The DNA tail moment was obtained about 5 μm after the exposure of the AgNPs prepared at increased citrate concentrations higher than 8×10^{-4} M and their supernatants, as seen in figure 9(b).

4. Discussions

In the Lee–Meisel method, the synthesis mechanism of the AgNPs consists of three main stages [5]. In the first stage, the Ag^{+} ion concentration in the suspension leads to the generation of AgNPs by stacking atomic silver. In the second stage, the clusters of Ag atoms produce numerous nuclei or

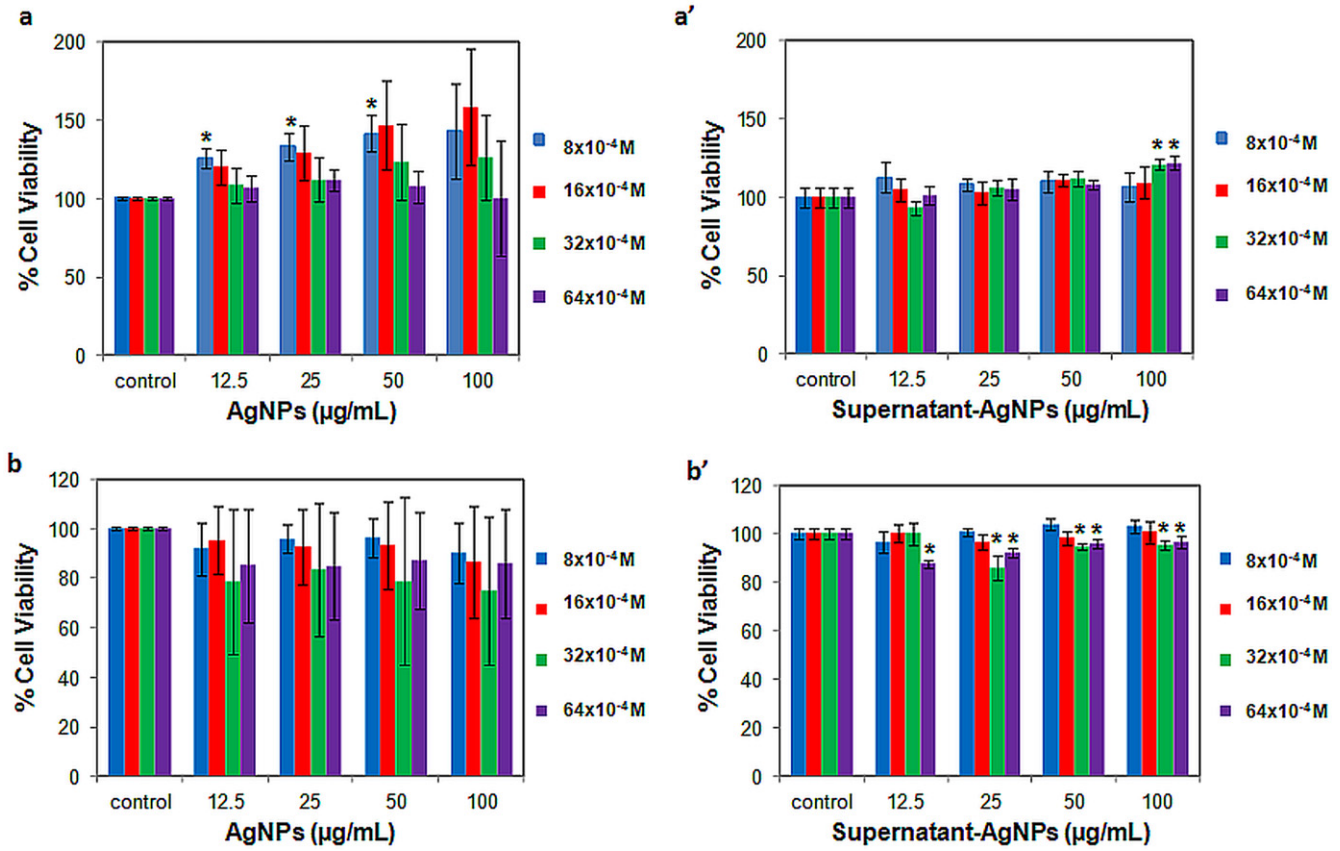

Figure 6. Cytotoxicity of colloidal AgNP suspension (a and b) and their respective supernatants (a′ and b′) prepared with increasing citrate concentration from 8×10^{-4} to 64×10^{-4} M after 24 h treatment of HDF (a and a′) and A549 (b and b′) cell lines. The data normalized to control values (no particle exposure), which were set as 100% cell viability. * Shows the significant results compared to the control $P < 0.05$ as obtained using Student's t-test.

seeds as reduced. As the nuclei are saturated in the suspension, their aggregates form the AgNPs in the final stage. The termination time influences the dispersibility of the nuclei and the size variation of the AgNPs [2]. Below the saturation threshold, aggregation of the nuclei to the AgNPs does not occur. Considering the effect of reaction time on the nucleation and the formation of the AgNPs, the effect of reaction time on size and toxicity was evaluated by changing the reaction time from 5 min to 50 min.

The UV-vis spectra indicate that the size of the AgNPs increases with increases in reaction time. Similar results were also observed in a study by Šileikaitė *et al*, where the effect of boiling time on the synthesis of AgNPs was investigated [33]. In addition, the seeds, which were formed during the nucleation step, broaden the UV-vis bands, as observed in a similar study [20]. A shoulder seen at around 350 nm on the UV-vis spectra in figure 1(a) is a consequence of plasmon absorption determined through Mie formulations, as specified earlier [8]. As discussed previously, when the reaction is quenched in the middle of the nucleation step, the number of AgNPs seeds is relatively large. When sufficient time is given for the reaction (50 min in this study), the polydispersity of the AgNPs decreases and only large particles are observed, meaning that both the nucleation and growth steps are totally complete, as can be seen clearly in the DLS spectra and TEM images in figure 1(b) and figure 2.

The citrate concentration in the suspension has the ability to control the agglomeration tendency of the AgNPs. The electrostatic repulsion between the AgNPs proportionally increases with increased citrate concentration, which controls AgNP growth and provides stability to the AgNPs [26, 27, 29, 45]. Thus, varying the citrate concentration was chosen as the second approach to verify its effects on the size and toxicity of AgNPs. While keeping the boiling time and the $AgNO_3$ concentration constant, the concentration of sodium citrate was gradually increased. The reaction time was chosen as 50 min, at which all Ag^+ ions reduced to AgNPs.

The blue shift on the UV-vis spectra of the AgNPs synthesized at increased citrate concentrations, indicating the NP size decrease. The DLS data also support this observation, but there are much smaller sizes of AgNPs along with large ones. Although citrate concentration provides stability to the AgNPs until a certain concentration, when an excess amount of citrate is used, the ionic strength of the solution increases, trigering the destabilization and coalescence of the AgNPs. The large particles that are formed as a result of the coalescence can also be observed in the TEM images in figure 4. Henglein *et al* explained that this situation is caused by the

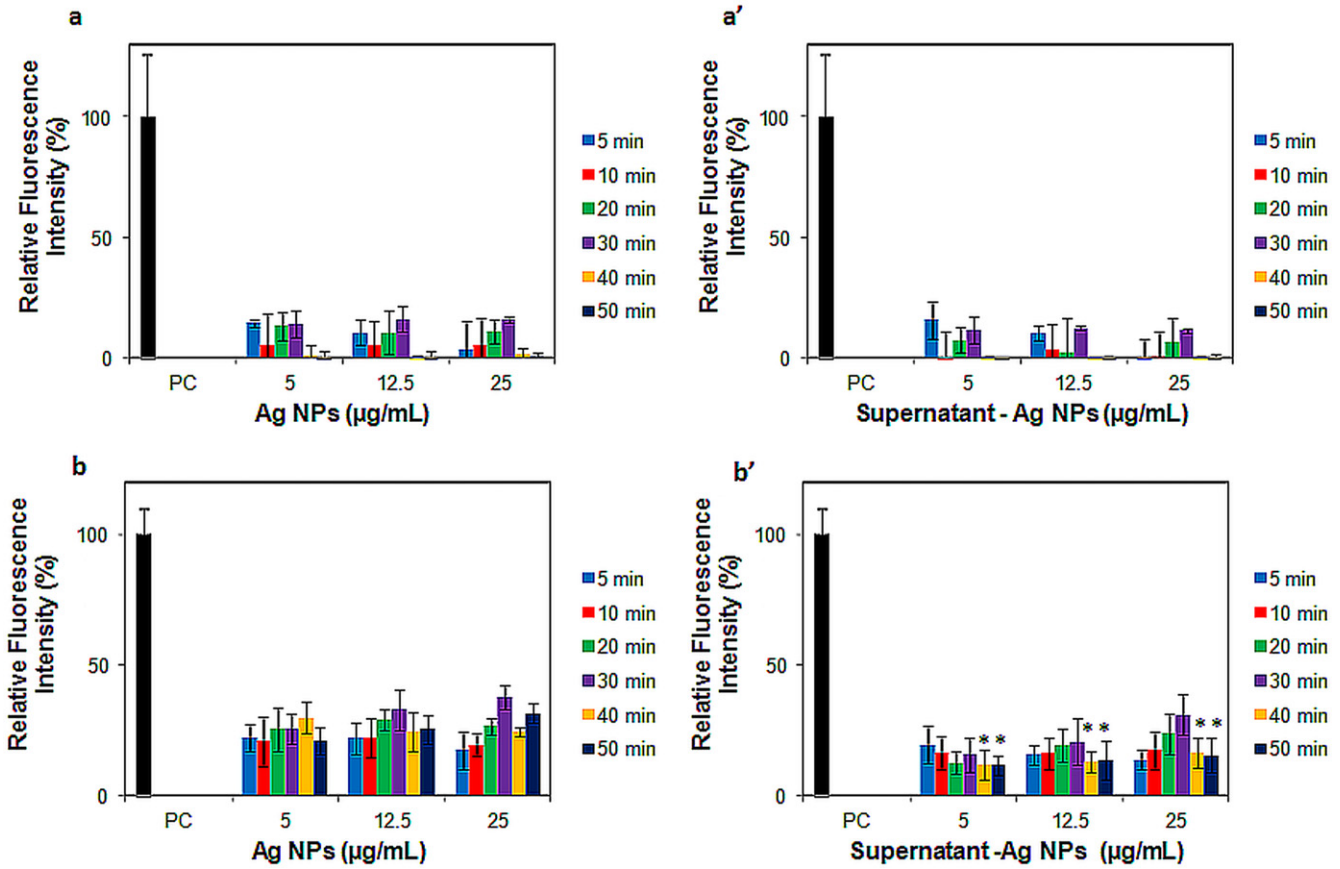

Figure 7. Effects of AgNP colloidal suspensions (a and b) and their respective supernatants (a′ and b′) prepared with increasing reaction time from 5 to 50 min after 6 h treatment on intracellular ROS production of HDF (a and a′) and A549 (b and b′) cells. The cells treated with the AgNPs *produced* DCF upon ROS production, which was measured by fluorescence spectrometry. TBHP was used as a positive control (PC). * Shows the significant decrease in intracellular ROS production after exposure of supernatant of AgNPs compared to the AgNPs exposure. $P < 0.05$ as obtained using Student's t-test.

coalescence of Ag clusters during the condensation step of AgNP formation [14].

The risk of human exposure to AgNPs is a big concern since their use in daily life has increased in recent years. The possible interaction of AgNPs and humans may occur through inhalation or dermal exposure, since they are now found in surface disinfectants, wound-healing products, anti-odor spray, and throat spray as an antimicrobial agent. The source of an AgNP's toxicity is related to its size, shape, reducing agent, and capacity to release Ag^+ ions [11, 22, 36]. Smaller AgNPs are up-taken by the cells easily via endocytosis, where they release Ag^+ ions into the cell and cause ROS generation [22]. The released Ag^+ ions are demonstrated to cause the ROS production, mitochondrial function disruption, and cell membrane damage [4, 6, 22]. In the literature, speculations about the toxicity of similar-sized AgNPs come from the diversity of their synthesis methods and reducing agents, which influence their stability, reactive surfaces, and capacity to release of Ag^+ ions [11, 22]. Gliga *et al* demonstrated the differences between the toxicity of the citrate- and PVP-coated 10 nm AgNPs in terms of their stability and capacity to release Ag^+ ions [11]. They claimed that PVP-coated AgNPs were more stable than the citrate-coated ones since the weakly bound citrate ions on an AgNP's surface could easily exchange with medium components compared to the strongly adsorbed noncharged larger PVP polymer. In other study, Li *et al* optimized the reaction conditions, and synthesized mono-dispersed and different but definite sized AgNPs in the range of 25 to 70 nm, using PVP as a reducing agent to demonstrate the toxicity of smaller-sized AgNPs [22]. However, Kim *et al* showed that the 100 nm AgNPs have greater toxicity than 10 nm AgNPs [18]. Another controversial issue is the variation of the exposure dose of the AgNPs during *in vitro* studies. Although the toxic concentration of AgNPs was reported as $10\,\mu g\,mL^{-1}$ by the National Institute for Occupational Safety and Health (NIOSH) (NIOSH, 2005), concentrations have existed in a wide range, up to $250\,\mu g\,mL^{-1}$, in most of the studies [11, 18, 22]. Herein the reason for the AgNPs' toxicity was linked to the synthesis conditions. The influence of the AgNPs' suspensions prepared via increasing reaction time and citrate concentration, and their perspective supernatant on AgNPs cytotoxicity induced ROS production and genotoxicity. When the reaction time increased, the number of AgNP seeds forming the larger particles decreased, as was previously discussed. This study demonstrated that the remaining number of seeds was proportional to the adverse effect of the AgNPs on cells due to their large reactive surfaces and tendency to release Ag^+ ions

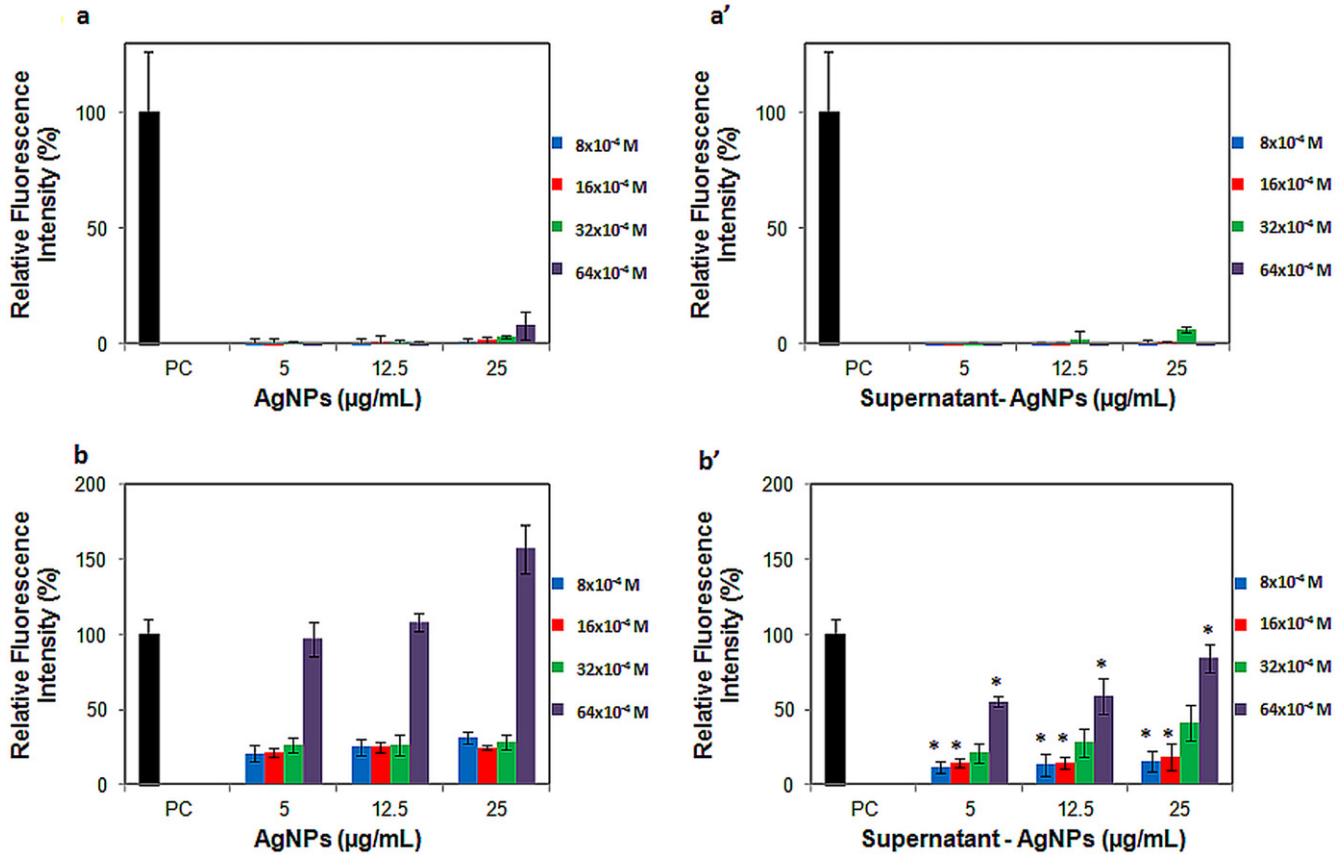

Figure 8. Effects of AgNP colloidal suspensions (a and b) and their respective supernatants (a′ and b′) prepared with increasing citrate concentration from 8×10^{-4} to 64×10^{-4} M after 6 h treatment on intracellular ROS production of HDF (a and a′) and A549 (b and b′) cell lines. The cells treated with the AgNPs produced DCF upon ROS production which was measured by fluorescence spectrometry. TBHP was used as a positive control (PC). * Shows the significant decrease in intracellular ROS production after exposure of supernatant of AgNPs compared to the AgNPs exposure. $P < 0.05$ as obtained using Student's t-test.

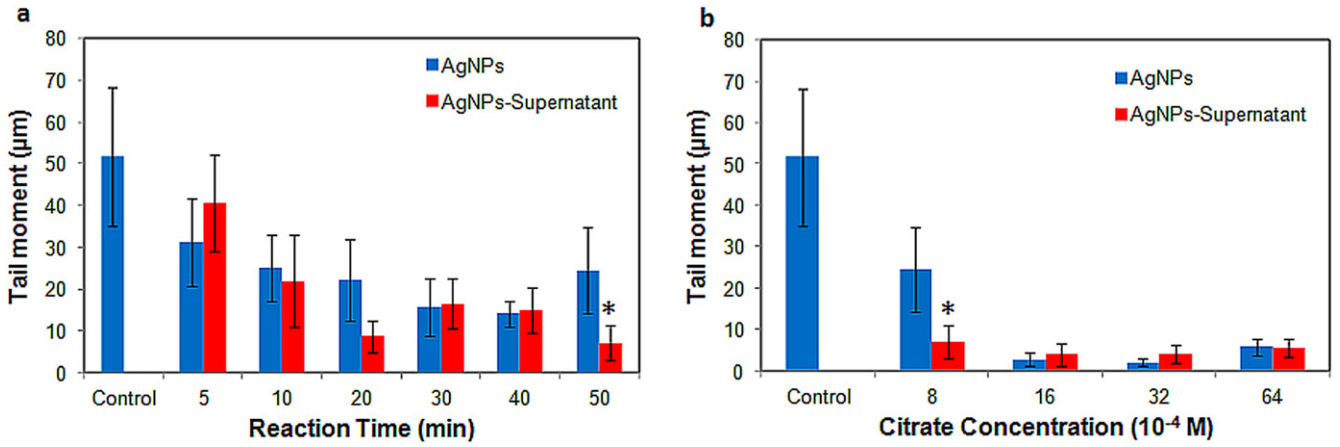

Figure 9. Genotoxicity of AgNP colloidal suspension and its supernatant of AgNPs prepared by (a) reaction time from 5 to 50 min and (b) increased citrate concentration from 8×10^{-4} to 64×10^{-4} M after 24 h treatment of A549 cells at 25 μg mL^{-1} concentration. The control represents hydrogen peroxide exposed cells. * Shows the significant results AgNPs exposure compared to exposure of supernatant of AgNPs. $P < 0.05$ as obtained using Student's t-test.

in the suspension. The AgNPs prepared with up to a 20 min reaction time largely destroyed the viability of cells due to the number of seeds, rather than the formed AgNPs in suspension. This result is supported by the significant decrease in cell viability after exposure to the supernatant of these AgNPs, where the seeds and Ag^+ ions could not be removed by centrifugation. After the exposure of the AgNPs prepared with 20- and 30 min reaction times, the cytotoxicity of the AgNPs decreased, but not completely, since the reaction was not completed, as was stated previously. A small amount of

the AgNP seeds may remain in the suspension, which caused the lost of cell viability after exposure to the AgNPs supernatant. Since the number of the reactive AgNP seeds decreased at 40 min and the reaction was substantially completed at 50 min, the exposure of the colloidal AgNP suspensions did not show any adverse effects on cell viability. During the evaluation of cell viability, a WST-1 assay was used, but the absorbance of the remaining AgNPs did not influence the absorbance of the WST-1 formazan. However, the results showed that the AgNPs prepared at 40 and 50 min have a positive effect on the viability of HDF cells. The reason for this can be explained based on the findings of our previous study, which showed that the citrate-reduced AgNPs with average 50 nm sizes improved wound healing through collagen synthesis and fibroblast proliferation in animal models [17]. When the citrate concentration was further increased to obtain more stable AgNPs, the resulting AgNP colloidal suspensions did not show significant adverse effects on cell viability. However, the increased citrate ions in the suspension decreased the A549 cell viability due to the selective negative effect of citrate on cancer cells [9]. No influence on HDF cell viability was observed at high citrate concentrations.

The major cause of the toxicity of AgNPs is reported to be the increased intracellular Ag^+ ion release, which disrupts mitochondrial function by interacting with the cystein residue of NADH dehydrogenase, thus initiating ROS production [3, 38]. ROS production significantly influences cells though oxidation of proteins and lipids, causing DNA damage. The HDF cells showed the generation of ROS after treatment with colloidal AgNP suspensions prepared up to 40 min; the ROS production was caused by the remaining AgNPs seeds and Ag^+ ions in the colloidal suspension. Their supernatants also induced a similar rate of ROS production. As was expected, the significant decrease in ROS production after exposure of the AgNPs prepared at 40 min and 50 min and their supernatant strongly supports the impact of AgNPs seeds and Ag^+ ions on ROS production.

The ROS levels obtained were two times higher in A549 cells compared to the HDF cells, demonstrating the cell-line-dependent action of the AgNPs. The exposure of the AgNPs' colloidal suspension prepared at increasing reaction times from 5 to 50 min did not induce a significant difference in ROS production in A549 cells. However, ROS production after exposure to the supernatant of the AgNPs prepared at 40 and 50 min decreased significantly. With the increase in reaction time, the number of Ag^+ ions, AgNP seeds, and the reactive surfaces changed, but the citrate ion concentration was constant during exposure. It is clear that the reason for the stable level of ROS production in A549 cells regardless of a change in the AgNPs type is the selective effect of citrate ions on the mitochondrial activity of A549 cancer cells [9].

The differential action of the AgNPs on the ROS production of the cells is clearly demonstrated by the results obtained after the exposure of the AgNPs prepared at increasing citrate concentrations. ROS production was not induced in HDF cells since the seeds in the suspension formed larger AgNPs at 50 min, and their reactive surfaces were coated with citrate ions, which were considered to be the reason for the induced ROS production in HDF cells. However, the ROS production significantly increased in A549 cells upon exposure to the AgNPs and their supernatant prepared with increased citrate concentrations. As it is well known, the citrate is a carbon source used by mitochondria for energy. The influence of sodium citrate on human lung fibroblast cells (MRC-5) and human lung cancer cells (A549) was reported by Farah *et al* [9], who claimed that citrate ions selectively kill the cancer cells, which explains the increased level of ROS production on A549 cells. This result suggests that both the AgNPs and the reducing agent have an influence on cells.

The genotoxicity of the AgNPs was evaluated on A549 cells at 25 μg mL^{-1} concentration since the viability of the A549 cells reached almost 0% after exposure of to the AgNPs and their supernatants prepared at 5 and 10 min; ROS production was at a maximum level after the exposure of A549 cells to the AgNPs prepared with 64×10^{-4} M citrate. Although the number of seeds and the reactive surface area varied with increased reaction time from 5 to 50 min, the average DNA damage was observed to be similar. In addition, the supernatant of these AgNPs showed similar results, with the exception of the supernatant of the AgNPs prepared at 50 min. However, when the citrate concentrations increased, the DNA damage significantly decreased even though ROS generation was observed to be greater. These results proved that the reactive surfaces of the AgNPs and the seeds were the major source of the genotoxicity. The citrate ions causing greater ROS production did not have much influence on the genotoxicity of the AgNPs on A549 cells.

5. Conclusions

Quenching the reaction during nucleation or the AgNP-formation step results in free AgNP seeds and Ag^+ ions in the suspension. These were major sources of toxicity originating from the colloidal suspension. The AgNP colloidal suspension prepared with an increasing citrate concentration was found to be less cytotoxic and genotoxic, even though it induced increased ROS production. The decreased toxicity was caused by the fact that higher concentrations of the citrate ions stabilized the AgNPs by blocking the reactive surfaces at an optimum concentration. The study reveals that the reaction time and the reducing agent concentration have a strong relationship with the particle size, polydispersity, agglomeration, and toxicity of the AgNPs. The most important outcome of the study is that both the size of AgNPs and their synthesis conditions have an impact on toxicity.

Acknowledgments

The authors acknowledge the financial support from European Council (FP7 Project NANOMICEX, GA no: 280713) partners involved in this project and Yeditepe University.

References

[1] Abou El-Nour K M, Eftaiha A, Al-Warthan A and Ammar R A 2010 Synthesis and applications of silver nanoparticles *Arab. J. Chem.* **3** 135–40

[2] Andhariya N, Pandey O and Chudasama B 2013 A growth kinetic study of ultrafine monodispersed silver nanoparticles *RSC Adv.* **3** 1127–36

[3] AshaRani P, Low Kah Mun G, Hande M P and Valiyaveettil S 2008 Cytotoxicity and genotoxicity of silver nanoparticles in human cells *ACS Nano* **3** 279–90

[4] Avalos A, Haza A I, Mateo D and Morales P 2014 Interactions of manufactured silver nanoparticles of different sizes with normal human dermal fibroblasts *Int. Wound J.* doi:10.1111/iwj.12244

[5] Chen D, Qiao X, Qiu X and Chen J 2009 Synthesis and electrical properties of uniform silver nanoparticles for electronic applications *J. Mater. Sci.* **44** 1076–81

[6] Chichova M, Shkodrova M, Vasileva P, Kirilova K and Doncheva-Stoimenova D 2014 Influence of silver nanoparticles on the activity of rat liver mitochondrial ATPase *J. Nanopart. Res.* **16** 1–14

[7] Chou K-S and Ren C-Y 2000 Synthesis of nanosized silver particles by chemical reduction method *Mater. Chem. Phys.* **64** 241–6

[8] Evanoff D D and Chumanov G 2004 Size-controlled synthesis of nanoparticles. 1.'silver-only' aqueous suspensions via hydrogen reduction *J. Phys. Chem.* B **108** 13948–56

[9] Farah I O, Lewis V L, Ayensu W K and Cameron J A 2013 Assessing the survival of MRC-5 and A549 cell lines upon exposure to pyruvic acid, sodium citrate and sodium bicarbonate *Biomed. Sci. Instrum.* **49** 109–16

[10] Ge C, Du J, Zhao L, Wang L, Liu Y, Li D, Yang Y, Zhou R, Zhao Y and Chai Z 2011 Binding of blood proteins to carbon nanotubes reduces cytotoxicity *Proc. Natl Acad. Sci. USA* **108** 16968–73

[11] Gliga A R, Skoglund S, Wallinder I O, Fadeel B and Karlsson H L 2014 Size-dependent cytotoxicity of silver nanoparticles in human lung cells: the role of cellular uptake, agglomeration and Ag release *Part. Fibre Toxicol.* **11** 11

[12] Gorityala B K, Ma J, Wang X, Chen P and Liu X-W 2010 Carbohydrate functionalized carbon nanotubes and their applications *Chem. Soc. Rev.* **39** 2925–34

[13] Haase A, Mantion A, Graf P, Plendl J, Thuenemann A, Meier W, Taubert A and Luch A 2012 A novel type of silver nanoparticles and their advantages in toxicity testing in cell culture systems *Arch. Toxicol.* **86** 1089–98

[14] Henglein A and Giersig M 1999 Formation of colloidal silver nanoparticles: capping action of citrate *J. Phys. Chem.* B **103** 9533–9

[15] Hu W, Peng C, Lv M, Li X, Zhang Y, Chen N, Fan C and Huang Q 2011 Protein corona-mediated mitigation of cytotoxicity of graphene oxide *ACS Nano* **5** 3693–700

[16] Kapoor S, Lawless D, Kennepohl P, Meisel D and Serpone N 1994 Reduction and aggregation of silver ions in aqueous gelatin solutions *Langmuir* **10** 3018–22

[17] Keleştemur S, Kilic E, Uslu Ü, Cumbul A, Ugur M, Akman S and Culha M 2012 Wound healing properties of modified silver nanoparticles and their distribution in mouse organs after topical application *Nanobiomed. Eng.* **4** 160–76

[18] Kim T H, Kim M, Park H S, Shin U S, Gong M S and Kim H W 2012 Size-dependent cellular toxicity of silver nanoparticles *J. Biodmed. Mater. Res.* Part A **100** 1033–43

[19] Kirchner C, Liedl T, Kudera S, Pellegrino T, Muñoz Javier A, Gaub H E, Stölzle S, Fertig N and Parak W J 2005 Cytotoxicity of colloidal CdSe and CdSe/ZnS nanoparticles *Nano Lett.* **5** 331–8

[20] Krylova G, Eremenko A, Smirnova N and Eustis S 2005 Structure and spectra of photochemically obtained nanosized silver particles in presence of modified porous silica *Int. J. Photoenergy* **7** 193–8

[21] Lee P and Meisel D 1982 Adsorption and surface-enhanced Raman of dyes on silver and gold sols *J. Phys. Chem.* **86** 3391–5

[22] Li L, Sun J, Li X, Zhang Y, Wang Z, Wang C, Dai J and Wang Q 2012 Controllable synthesis of monodispersed silver nanoparticles as standards for quantitative assessment of their cytotoxicity *Biomaterials* **33** 1714–21

[23] Li Y, Qian F, Xiang J and Lieber C M 2006 Nanowire electronic and optoelectronic devices *Mater. Today* **9** 18–27

[24] Liu W, Wu Y, Wang C, Li H C, Wang T, Liao C Y, Cui L, Zhou Q F, Yan B and Jiang G B 2010 Impact of silver nanoparticles on human cells: effect of particle size *Nanotoxicology* **4** 319–30

[25] Merga G, Wilson R, Lynn G, Milosavljevic B H and Meisel D 2007 Redox catalysis on 'naked' silver nanoparticles *J. Phys. Chem.* C **111** 12220–6

[26] Mpourmpakis G and Vlachos D G 2008 Insights into the early stages of metal nanoparticle formation via first-principle calculations: the roles of citrate and water *Langmuir* **24** 7465–73

[27] Mpourmpakis G and Vlachos D G 2009 Growth mechanisms of metal nanoparticles via first principles *Phys. Rev. Lett.* **102** 155505

[28] Nickel U, zu Castell A, Pöppl K and Schneider S 2000 A silver colloid produced by reduction with hydrazine as support for highly sensitive surface-enhanced Raman spectroscopy *Langmuir* **16** 9087–91

[29] Pillai Z S and Kamat P V 2004 What factors control the size and shape of silver nanoparticles in the citrate ion reduction method? *J. Phys. Chem.* B **108** 945–51

[30] Salerno M, Krenn J, Lamprecht B, Schider G, Ditlbacher H, Felidj N, Leitner A and Aussenegg F 2002 Plasmon polaritons in metal nanostructures: the optoelectronic route to nanotechnology *Optoelectron. Rev.* **10** 217–24

[31] Sharma V K, Yngard R A and Lin Y 2009 Silver nanoparticles: green synthesis and their antimicrobial activities *Adv. Colloid Interface Sci.* **145** 83–96

[32] Shirtcliffe N, Nickel U and Schneider S 1999 Reproducible preparation of silver sols with small particle size using borohydride reduction: for use as nuclei for preparation of larger particles *J. Colloid Interface Sci.* **211** 122–9

[33] Šileikaitė A, Puišo J, Prosyčevas I and Tamulevičius S 2009 Investigation of silver nanoparticles formation kinetics during reduction of silver nitrate with sodium citrate *Mater. Sci.* **15** 21–7

[34] Sondi I, Goia D V and Matijević E 2003 Preparation of highly concentrated stable dispersions of uniform silver nanoparticles *J. Colloid Interface Sci.* **260** 75–81

[35] Sun Y, Gates B, Mayers B and Xia Y 2002 Crystalline silver nanowires by soft solution processing *Nano Lett.* **2** 165–8

[36] Sur I, Altunbek M, Kahraman M and Culha M 2012 The influence of the surface chemistry of silver nanoparticles on cell death *Nanotechnology* **23** 375102

[37] Tao A, Sinsermsuksakul P and Yang P 2006 Polyhedral silver nanocrystals with distinct scattering signatures *Angew. Chem., Int. Ed. Engl.* **45** 4597–601

[38] Teodoro J S, Simões A M, Duarte F V, Rolo A P, Murdoch R C, Hussain S M and Palmeira C M 2011 Assessment of the toxicity of silver nanoparticles *in vitro*: a mitochondrial perspective *Toxicol. in Vitro* **25** 664–70

[39] Wan Y, Guo Z, Jiang X, Fang K, Lu X, Zhang Y and Gu N 2013 Quasi-spherical silver nanoparticles: aqueous synthesis and size control by the seed-mediated Lee–Meisel method *J. Colloid Interface Sci.* **394** 263–8

[40] Wang L, Wang F and Chen D 2008 Fabrication and characterization of silver/polystyrene nanospheres with more complete coverage of silver nano-shell *Mater. Lett.* **62** 2153–6
[41] Wei L, Tang J, Zhang Z, Chen Y, Zhou G and Xi T 2010 Investigation of the cytotoxicity mechanism of silver nanoparticles in vitro *Biomed. Mater.* **5** 044103
[42] Wiley B, Sun Y, Mayers B and Xia Y 2005 Shape-controlled synthesis of metal nanostructures: the case of silver *Chem.-A Eur. J.* **11** 454–63
[43] Xia T, Zhao Y, Sager T, George S, Pokhrel S, Li N, Schoenfeld D, Meng H, Lin S and Wang X 2011 Decreased dissolution of ZnO by iron doping yields nanoparticles with reduced toxicity in the rodent lung and zebrafish embryos *ACS Nano* **5** 1223–35
[44] Xiong J, Wang Y, Xue Q and Wu X 2011 Synthesis of highly stable dispersions of nanosized copper particles using L-ascorbic acid *Green Chem.* **13** 900–4
[45] Yin H, Yamamoto T, Wada Y and Yanagida S 2004 Large-scale and size-controlled synthesis of silver nanoparticles under microwave irradiation *Mater. Chem. Phys.* **83** 66–70